Partitioning the phase space in a natural way for scattering systems

A. Emmanouilidou[1] and C. Jung[2]
[1]*Center for Nonlinear Science, School of Physics, Georgia Institute of Technology, Atlanta, Georgia, 30332-0430, USA*
[2]*Centro de Ciencias Fisicas, UNAM, Apdo postal 48-3, 62251 Cuernavaca, Mexico*
(Received 12 September 2005; published 30 January 2006)

In this paper, we demonstrate a recent procedure for the construction of a symbolic dynamics for open systems by applying it to a model potential, the driven inverted Gaussian, which has proven very useful in describing laser-atom interaction. The symbolic dynamics and the corresponding partition of the Poincaré map are natural from the point of view of an asymptotic observer since the resulting branching tree coincides with the one extracted from the scattering functions. In general, the whole procedure is approximate because it only describes the globally unstable part of the chaotic invariant set, that is, the part that can be seen by an asymptotic observer in scattering data. It ignores Kolmogorov-Arnold-Moser islands and their fractal surroundings.

DOI: 10.1103/PhysRevE.73.016219 PACS number(s): 05.45.−a

I. INTRODUCTION

Finding a symbolic dynamics is the most global way of describing a chaotic system. The symbolic dynamics corresponds to a partitioning of the phase space in cells. With a symbolic dynamics, every trajectory can be labeled by a symbol sequence that corresponds to the sequence of the partition cells visited by this trajectory. We consider systems that can be cast into some iterated map on a two-dimensional domain. In this map, the chaotic set is represented by a version of Smale's horseshoe [1], which in most cases is an incomplete one. Developing a symbolic dynamics for these systems is equivalent to partitioning the fundamental area R of the horseshoe, that is, the area that covers the chaotic set.

For incomplete horseshoes, pruning [2] sets in and the construction of a symbolic dynamics becomes a difficult task. In previous studies [3], a symbolic dynamics has been developed that partitions the phase space using lines of maximal folding of the horseshoe as division lines of the partition cells. An improved version [4] of the originally developed symbolic dynamics uses, in addition, symmetry lines as division lines to handle Kolmogorov-Arnold-Moser (KAM) islands. If one is only interested in finding measures of chaos, then the previously developed symbolic dynamics, with the use of the thermodynamic formalism [5], allows one to do so. However, if one is interested in describing scattering systems and, thus, in obtaining all information relevant to scattering trajectories, then it is also important to partition the phase space in a "natural" way from the scattering perspective. Specifically, the scattering functions of chaotic systems have a pattern of singularities and intervals of continuity. When we refer to a natural way of partitioning the phase space, we mean that the partition has to be such that all scattering trajectories that have initial conditions in the same interval of continuity of the scattering function are labeled by the same symbol sequence. More specifically, the hierarchical structure of these intervals of continuity can be cast in the form of a branching tree. The structure of this branching tree is completely determined by the intersection pattern between the stable manifolds and the local segment of the unstable manifold of the outer fixed points of the Poincaré map. Iteration step after iteration step of the map, new gaps are cut out of this local segment of the unstable manifold and these gaps correspond one to one to the intervals of continuity of the scattering functions. It is clear that if scattering trajectories in the same interval of continuity are to be labeled by the same symbol sequence, then the division lines of the partition cells must be related to the manifolds of the outermost fixed points.

We have already developed a general algorithm for partitioning the Poincaré map that is natural (in the sense mentioned above) for scattering systems that can be cast in a two-dimensional Poincaré map. Our method is described in technical detail in Ref. [6]. However, we point out, that unlike the previously developed symbolic dynamics, our partition does not account for KAM islands. As with any scattering-based treatment of a system, our symbolic dynamics can only take into account the part of the system that is accessible to the outside world and can be seen by an asymptotic observer. Therefore, our partition takes into account only the outer unstable part of the horseshoe and completely ignores the KAM islands. Consequently, near the fractal surface of a KAM island and its surrounding secondary structures, our partition is approximate.

In the current work, we first explain and motivate the two principles on which our partition is based. We discuss how the first principle assures that scattering trajectories from the same interval of continuity are described by the same symbol sequence. We also explain how the second one results in a symbolic dynamic with grammatical rules of length one, that is, the simplest symbolic dynamic. In addition, we explain, in detail, how one extracts from our partition all the relevant scattering information. That is, we discuss how the chaotic saddle (chaotic set) "transfers" the scattering trajectories with initial conditions in a given interval of continuity through the interaction region to the asymptotic one. Specifically, we show how one can find, using our partition, the number of times a trajectory steps inside the fundamental area R of the Poincaré map, the sequence of partition cells the trajectory steps in, inside the area R, and whether the trajectory reflects or transmits. We illustrate how to extract all the scattering information from our partition in the con-

text of a one-dimensional inverted Gaussian potential driven by a laser field. This model potential has been successfully used in previous studies to explain a variety of aspects of the laser-atom interactions [7].

Our general scheme of partitioning the phase space and obtaining the relevant scattering information is based on the intersection pattern of stable and unstable manifolds. We believe that this general scheme will facilitate the understanding of the mechanisms governing chaotic transport in a variety of systems. The way a description of scattering functions in terms of the intersection pattern of the stable and unstable manifolds of the relevant fixed points leads to an understanding of the transport through the chaotic saddle is nicely illustrated in a recent classical study of the hydrogen atom in parallel electric and magnetic fields excited by a short laser pulse [8].

II. MODEL

We illustrate the principles of our partition using a one-dimensional inverted Gaussian atomic potential in the presence of a strong time-periodic electric field. The electric field $E(t)=E_0\sin(\omega t)$ ($T=2\pi/\omega$ is the period of the field) is treated within the dipole approximation as a monochromatic infinite plane wave linearly polarized along the direction of the incident electron. This potential has offered considerable insight into the laser-atom interactions [7]. The Hamiltonian in the Kramers-Henneberger reference frame (the frame that oscillates with a free electron in the time-periodic field) [9] is

$$H(x,t)=\frac{p^2}{2}-V_0e^{-\{[x+\alpha(t)]/\delta\}^2}, \tag{1}$$

where $\alpha(t)=\alpha_0\sin(\omega t)$ is the classical displacement of a free electron from its center of oscillation in the time-periodic electric field $E(t)$ with $\alpha_0=-qE_0/\omega^2$ (q is the particle charge which for the electron is $q=-1$ a.u.). We use atomic units throughout the paper if not otherwise stated. Next, we transform Eq. (1) to a two-degree-of-freedom time-independent system, where the total energy E of the system is conserved, as follows:

$$H=\frac{p^2}{2}-V_0e^{-\{[x+\alpha_0\sin(\phi)]/\delta\}^2}+\omega I. \tag{2}$$

I and ϕ are, respectively, the action-angle variables of the driving field. Using Eq. (2), we find from Hamilton's equations of motion that $\phi=\omega t$. In the Secs. II A and II B all our calculations are performed with the values $V_0=0.270\,35$ a.u. and $\delta=2$ a.u. assigned to the parameters of the inverted Gaussian potential. The frequency of the time-periodic field ω and the amplitude of the field α_0 are taken constant and equal to 0.65 a.u. and 0. 9 a.u., respectively [10].

A. Chaotic invariant set

The chaotic invariant set is usually represented by a horseshoe construction in an appropriate Poincaré surface of section. In the case of the well-known Smale horseshoe, the construction is done by stretching a fundamental region R and folding it onto the original region [1,12]. The boundaries of R are given by segments of the invariant manifolds of the outer fixed points of the system. The system under consideration has three period-1 orbits (fixed points). The inner fixed point is an elliptic one. The two outer fixed points are located at $x\to\pm\infty$ [10]. As $x\to+\infty$, the invariant stable and unstable manifolds of the outer fixed point C (see Fig. 1), converge to the same manifold (eigenvector), with $p=0$, where p is the momentum. The same is true for the manifolds of the fixed point A at $x\to-\infty$. Thus, in a small neighborhood around them, the outer fixed points behave as parabolic ones. That is, the tangent map at $x\to\pm\infty$ has a degenerate eigenvalue equal to 1 (one eigenvector) [11]. However, globally, the outer fixed points behave as unstable ones; that is, they produce invariant manifolds of the same topology as that produced by hyperbolic fixed points. The two fixed points at $x\to\pm\infty$ have invariant manifolds that go into the interior region and trace out the horseshoe that is under investigation. The horseshoes shown in this paper are traced by the fixed points at $x\to\pm\infty$, as explained below. For this driven system, the Poincaré map is a stroboscopic plot. That is, we plot x and p every complete period of the field, solving Hamilton's equations of motion. The static Gaussian potential e^{-x^2/δ^2} is symmetric under the reflection $x\to-x$, but this symmetry is destroyed by the interaction with the laser field, which is accounted for by including the $\alpha(t)/\delta$ term as $e^{-\{[x+\alpha(t)]/\delta\}^2}$. However, the potential remains invariant under the simultaneous operation $x\to-x$ and $t\to-t$. In addition, the complete Hamiltonian has the symmetry $p\to-p$. We need to consider how all of the above-mentioned symmetry properties manifest themselves in the Poincaré map, which in our case is a stroboscopic map, when using the Hamiltonian in the version given in Eq. (1). The appearance of the above-mentioned symmetries depends on our particular choice either of the constant τ in the intersection condition $t_n=\tau+nT$, when using Eq. (1) to construct the Poincaré map, or the corresponding value of Φ in the intersection condition $\phi=\Phi \bmod 2\pi$, when using Eq. (2) to construct the Poincaré map. For time-independent systems, the transformation $p\to-p$ usually corresponds to the time-reversal symmetry and amounts to in-

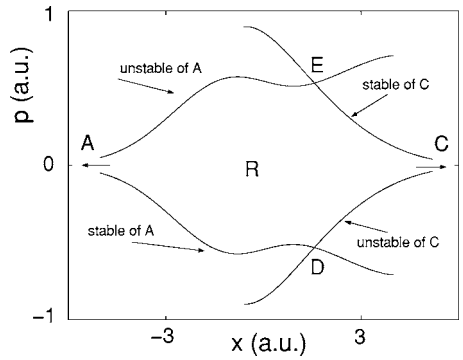

FIG. 1. The fundamental region R is formed by the unstable manifold of the fixed point A, segment AE, by the stable manifold of the fixed point C, segment CE, by the unstable manifold of the fixed point C, segment CD, and the stable manifold of the fixed point A, segment AD.

terchanging the stable with the unstable manifolds in the map and vice versa. This property is also valid in our case for the particular choice $\Phi = \pm \pi/2$. However, for this choice of the Poincaré surface of section, there is no reflection symmetry, $x \to -x$, in the map. On the other hand, for the choice $\Phi = 0$ the left-right symmetry is conserved, but then the time-reversal symmetry is not simply expressed as the $p \to -p$ reflection. For the system under consideration, the invariant set of the system is described by a ternary (three fixed points) asymmetric horseshoe construction. That is, the underlying structure of the scattering functions for electrons incident from the right and/or left is described by two different views right and/or left of the same horseshoe construction. The reason we consider the invariant manifolds of the outer fixed points is that these are the manifolds that are "seen" by the scattering trajectories and, thus, have an effect on the scattering functions, see Fig. 4 in Ref. [10]. In the following, we choose $\Phi = \pi/2$ in order to get the stable manifolds simply as the mirror images of the unstable manifolds under the $p \to -p$ reflection. It is important to realize that the symmetries of the system do not depend at all on the particular choice of the Poincaré surface of section. What the particular choice of the surface of section does is to determine the way the real symmetries of the system appear in the Poincaré map.

Let us now obtain the right view of the hierarchical structure of the horseshoe construction that underlies scattering for electrons incident from the right. The fundamental area R, see Fig. 1, is defined by the zero-order tendrils as well as an infinite number of preimages (images) of the unstable (stable) invariant manifolds, respectively. We now add one iteration step of the stable manifolds. That is, using Hamilton's equations of motion for the Hamiltonian given in Eq. (2), we propagate the points on the segments of the stable manifolds, AD and EC in Fig. 1, backwards in time for one period of the driving field. (To obtain the tendrils of the unstable manifolds we propagate forward in time.) The intersection of the first image, first-order tendrils, of the stable manifolds with the unstable manifold of the fixed point C, segment CD in Fig. 1, reveals the first-order gap G_1^s, see Fig. 2. The intersection with the unstable manifold of one more iteration step of the stable manifolds reveals the second order gaps G_2^s, see Fig. 2. Thus, the gap G_n^s is the area enclosed by the nth-order tendril of the stable manifold and the boundary of the fundamental area R. A point that lies in G_n^s is mapped out of the fundamental region after n applications of the map; it is, thus, of hierarchy level n. These gaps play an important role because they are areas that are not needed to cover the invariant set. No higher-level tendrils of the invariant manifolds will ever enter such gaps. Thus, with each iteration step, one further tendril of the stable manifolds is added and one further level of hierarchy of these gaps is displayed [13]. We therefore see the construction scheme of the horseshoe by going from one level of hierarchy to the next. We note that the term "gaps" corresponds to what is known as lobes in fluid-transport problems [14]. In particular, the gaps correspond to those lobes that are inside the area R. In a similar way, we construct the left view of the hierarchical structure of the horseshoe construction that underlies scattering for electrons incident from the left, see Fig. 2. The intersection points of the stable manifolds with the unstable manifolds of the outer fixed points, seen in Fig. 2 are the so-called homoclinic and heteroclinic points for intersecting manifolds corresponding to the same (homoclinic) or different (heteroclinic) fixed points. These homoclinic and heteroclinic intersections underlie the classical chaotic scattering.

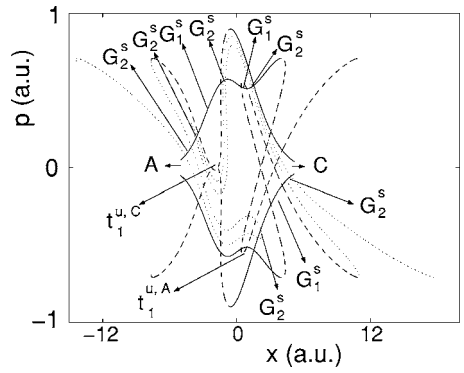

FIG. 2. Horseshoe construction up to hierarchy level two on the Poincaré surface of section $\Phi = \pi/2$. The solid lines indicate tendrils of order zero, the dashed lines indicate tendrils of order one, and the dotted lines indicate tendrils of order two. The gaps G_n^s on the bottom right and top left are formed by intersections of the stable manifolds of fixed points A and C with the local segment of the unstable manifold of fixed point C/A, that is, CD/AE. These intersections describe the right view and left view of the horseshoe construction. $t_1^{u,A}$ indicates the first-order inner tendril of the unstable manifold of the fixed point A. $t_1^{u,C}$ indicates the first-order inner tendril of the unstable manifold of the fixed point C.

B. Scattering functions and branching trees

Thus far, we have described the topology and hierarchical structure of the chaotic invariant set. Since, our partition is a natural one for scattering trajectories, the question arises as to how the hierarchical structure of the chaotic set is related to the hierarchical structure of the scattering functions. First, we note that the scattering functions give properties of the final electron asymptotes as a function of the incoming electron asymptotes. In the case of classical chaotic scattering, the scattering functions have a fractal set of singularities. This fractal set of singularities is the result of the intersection of the incoming electron asymptotes with the stable manifolds of the underlying chaotic invariant set. That is, when the scattering electron trajectory starts exactly on the stable manifold of the chaotic invariant set, it stays on the chaotic set forever, resulting in a singularity of the scattering function. Furthermore, the structure of the set of singularities is the same as the structure of the chaotic invariant set [13]. Thus, the reason we present the hierarchical structure of the chaotic set is that it is exactly the same as that of the scattering functions [10]. An example of a scattering function is the time delay of the incident electron as a function of the initial momentum [10], see Fig. 3. The incident electron delays, in the case of the driven Gaussian, due to the interplay of the inverted Gaussian potential with the driving field.

The hierarchical structure of the scattering functions can be expressed in the form of a branching tree. Let us first explain how to obtain a branching tree [13], which describes

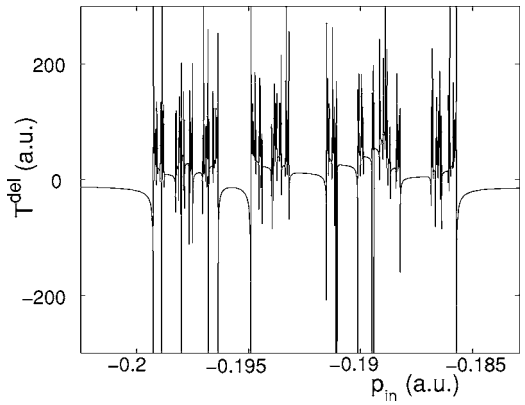

FIG. 3. Time-delay function as a function of the initial momentum for a set of initial conditions. The initial conditions are a line on the Poincaré surface of section that intersects the stable manifold of fixed point A in the right asymptotic region. This line of initial conditions is defined by $\Phi_{(t=0)}=\pi/2$, and the edge points $(x_1,p_1)=(10.5,-0.2025)$ and $(x_2,p_2)=(10.823,-0.1829)$.

the right view of the horseshoe construction for scattering from the right. We will use information developed in Sec. II A. (Describing how to obtain a branching tree has already been explained in Ref. [10], but we include it in the current paper for clarity purposes.) First, let us consider the interval I_1^0, which corresponds to the local segment of the unstable manifold CD of the fixed point C, see Fig. 4. This is the first step in the construction of the branching tree and corresponds to hierarchy level $n=0$. In the second step, hierarchy level $n=1$, the first-order tendril of the stable manifold of the fixed point A cuts the interval (s_0,s_1) out of I_1^0 and leaves two intervals I_1^1 (the segment of CD from D to s_0) and I_2^1 (the segment of CD from s_1 to C). In the third step, hierarchy level $n=2$, the second-order tendril of the stable manifold of the fixed point A cuts the interval (s_4,s_5) out of I_2^1 and leaves two intervals, I_{21}^2 (the segment of CD from s_1 to s_4) and I_{22}^2 (the segment of CD from s_5 to C). In the same step (the same iteration), the second-order tendril of the stable manifold of

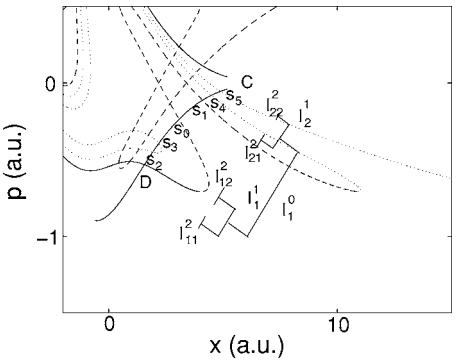

FIG. 4. Construction of the branching tree for scattering from the right. The first-order gap G_1^s reduces the initial interval I_1^0, at hierarchy level $n=0$, down to the two intervals I_1^1 and I_2^1. Note that for the scattering functions, we obtain exactly the same branching tree as for the chaotic invariant set. For the scattering functions, instead of the gaps it is the intervals of continuity that are cut out from the original interval in a Cantor-set structure.

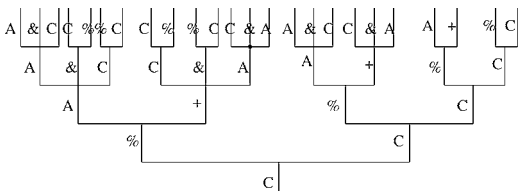

FIG. 5. Branching tree and its encoding for scattering trajectories coming in from the right.

the fixed point C cuts the interval (s_2,s_3) out of I_1^1 and leaves two intervals, I_{11}^2 (the segment of CD from D to s_2) and I_{12}^2 (the segment of CD from s_3 to s_0). Continuing this process, we obtain the branching tree shown in Fig. 5, that is, we obtain the topology of the branching tree. The way we obtain the symbol sequences in Figs. 5 and 6 will be explained later. In a similar way, we construct the branching tree that describes the left view of the horseshoe construction for scattering from the left, see Fig. 6. The hierarchical structure of these branching trees is the same as the hierarchical structure of the chaotic invariant set.

Thus far, we have shown how the branching trees, which describe the hierarchical structure of the scattering functions, are completely determined by the topology of the chaotic invariant set. If one is only interested in obtaining measures of chaos, then it is not difficult to develop a set of grammatical rules that describe the branching trees in Figs. 5 and 6. There is actually an infinite number of "encodings" one can develop to encode the trees. However, the important question is whether or not there is a symbolic encoding of the branching trees that is natural from the scattering perspective. That means that we are actually interested in developing a scheme of partitioning the area R in cells so that the encoding of our trees describes how each scattering trajectory visits the partition cells in the interaction region. Developing such a partition scheme is a nontrivial task. We have already developed such a general partition scheme valid for all two-degree-of-freedom systems in the form of an algorithm, as described in technical detail in Ref. [6]. In the current work, we first explain and motivate the two principles of our partition. We

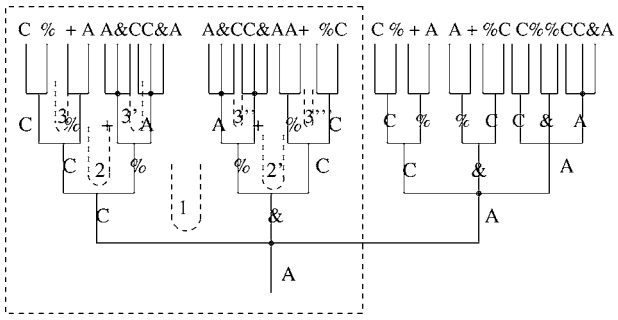

FIG. 6. Branching tree and its symbolic encoding for scattering trajectories coming in from the left. We also draw the gaps 1, 2, 2′, 3, 3′,3″, and 3‴ of the chaotic saddle, which correspond to the intervals of continuity labeled by $A[\&,C]$, $AC\ [\%,C]$, $A\&[C,\%]$, $ACC[\%,C]$, $AC\%[A,+]$, $A\&\%[+,A]$ and $A\&C[C,\%]$, respectively, to better clarify the discussion in the fourth section of Fig. 11. These intervals of continuity correspond to those parts of the segment E in Fig. 11 that are labeled as 1, 2, 2′, 3, 3′,3″, and 3‴.

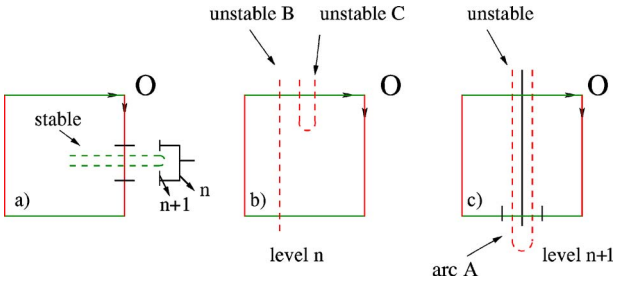

FIG. 7. (Color online) The preimage of the arc A can have either one of the qualitative structures shown as segments B and C in (b). The $(n+1)$th preimage of the arc A is the segment of the unstable manifold of the fixed point O contained between the black lines in (a). The $(n+1)$th preimage of the segment of the stable manifold contained in between the black lines in (c) is the stable gap in (a).

then show why this partition is a natural one for scattering systems. That is, we show that for each scattering trajectory in the same interval of continuity our partition gives the following information: (i) the number of times the trajectory steps inside the fundamental region before it is reflected or transmitted, (ii) the sequence of partition cells each scattering trajectory steps in, in the area R, and (iii) whether the trajectory reflects or transmits.

III. PRINCIPLES OF THE PARTITION

We first explain, in detail, the basic principles of our method for partitioning the phase space, a method that is applicable to any incomplete horseshoe on a Poincaré map defined on a two-dimensional domain. Our goal is to describe the behavior of scattering trajectories. To do so, the symbolic dynamics one obtains as a result of our method of partitioning the phase space must encode the branching trees. In addition, our partitioning must be such that trajectories from different intervals of continuity are described by different symbol sequences while trajectories from the same interval are described by the same symbol sequence. A natural requirement our partition must satisfy is that the symbol sequence labeling the trajectories in an interval of continuity must have length equal to the hierarchical level of the interval. As we explain later, this implies that trajectories from a certain interval of continuity step inside the fundamental area R as many times as the hierarchical level of the interval of continuity -1.

The above-described requirements are satisfied by partitioning the phase space according to the following two principles:

Principle 1. If an arc of the unstable manifold (which is the boundary of a gap) exits R and reenters R, then the two partition cells that this arc connects must be different; that is, they must belong to different symbol values, provided that the preimage of the segment that exits R has been completely inside R.

We illustrate principle 1 using Fig. 7. Principle 1 states that if a gap of the unstable manifold cuts the area R completely, as shown in Fig. 7(c) and the segment of the unstable manifold that is outside R [labeled as arc A in Fig. 7(c)] has a preimage inside R, then a different partition cell is introduced on either side of the unstable gap in Fig. 7(c). The preimage of the arc A can have either one of the two qualitative structures shown as segments B and C in Fig. 7(b). Using Fig. 7(a), we now explain how the above division line, which introduces different cells on either side of the unstable gap, guarantees that trajectories in different intervals of continuity are labeled by different symbol sequences. First, it is important to realize that the branching tree of the hierarchical structure of the scattering trajectories depicts the way the stable manifolds of the outer fixed points intersect the local segment of the unstable manifold of the outer fixed point that lies on the same side as the one from which the scattering trajectories start. Let us consider trajectories initiated on the right asymptotic side, then the relevant local unstable manifold is that of the fixed point O in Fig. 7(a). The $(n+1)$th preimage of the unstable gap in Fig. 7(c) is the segment of the local unstable manifold in Fig. 7(a) that is bounded by the black lines. The segment of the stable manifold intersected by the unstable gap in Fig. 7(c) and bounded by the black lines has as $(n+1)$th preimage the stable gap indicated in Fig. 7(a). Note, the reciprocal behavior of the segments of the stable and unstable manifolds in Figs. 7(a) and 7(c). That is, the segment of the stable manifold bounded by the black lines in Fig. 7(c) has a $(n+1)$th preimage, which is a stable gap as shown in Fig. 7(a). At the same time, the unstable gap in Fig. 7(c) has a $(n+1)$th preimage, which is the segment of the unstable manifold bounded by the black lines in Fig. 7(a). The intersection of the local unstable segment by the stable gap in Fig. 7(a) corresponds to the part of the branching tree shown in Fig. 7(a). As we go from level n to $n+1$ in the branching tree, two different symbol values have to be introduced for the two segments of the unstable manifold that remain after it is intersected by the stable gap. Introducing a division line inside the gap, and, thus, different partition cells on either side of the unstable gap in Fig. 7(c), guarantees that at level $n+1$ two different symbol values are used to describe the two branches of the tree in Fig. 7(a). These two branches of the tree correspond to two different parts that are unresolved at level $n+1$. Thus introducing a division line guarantees that trajectories that are in different intervals of continuity are labeled by different symbol sequences.

Principle 2. A division line is introduced between two areas inside of R, where the arcs of unstable gaps have qualitatively different behavior. Specifically, consider first the following scenario: R has two stable sides and there are segments of unstable gaps in R that connect one of these stable sides with the other one. In addition, there are segments of unstable manifolds that start on one of these sides and return to the same side. It can be the case that these latter arcs wind around some incomplete unstable gap of a lower level or that the arc itself is such an incomplete gap, such as segment C in Fig. 7(b). These two different types of behavior must be separated by introducing a division line as their boundary. A second scenario of areas having qualitative different behavior is when some arcs wind around a gap that does not cut through R completely, and at the same time, there are other arcs winding around a different gap that also do not cut through R completely. These two qualitatively different areas must also be separated by a division line.

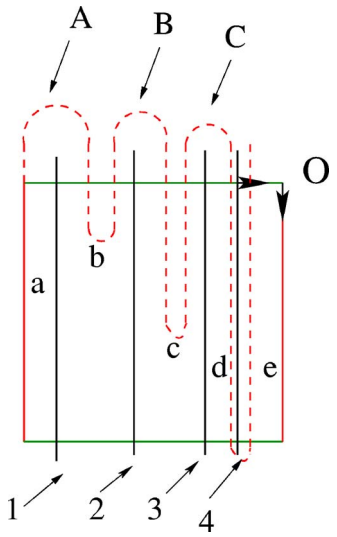

FIG. 8. (Color online) In this figure, we assume that C is the image of B and the second image of A. The division line 4 is introduced according to principle 1. Division lines 1, 2, and 3 are introduced according to principle 2.

Principle 2 guarantees that we obtain the simplest grammatical rules, that is, rules of length one. According to the first scenario of principle 2, we must introduce division lines 3 and 1 in Fig. 8, while according to the second scenario of principle 2 the division line 2 is introduced. Division line 4 is introduced according to principle 1. Similarly, as in the case of principle 1, the intersection of the unstable arc C with the stable manifold in Fig. 8, will have a, let us say, mth preimage similar to the one shown in Fig. 7(a). Similarly, the intersection of the unstable arc B with the stable manifold has a $(m-1)$th preimage similar to the one in Fig. 7(a), while the intersection of the unstable arc A with the stable manifold has a $(m-2)$th preimage similar to the one in Fig. 7(a). Each one of these preimages corresponds to a part of the branching tree as that shown in Fig. 7(a). Division lines 2 and 3 are not necessary because the above-mentioned preimages are of different hierarchical levels, and thus, the scattering trajectories inside the corresponding intervals of continuity have been separated at different hierarchical levels. Consequently, instead of introducing the three cells b,c, and d in Fig. 8, we could only introduce one, let us call it a'. However, in the case that no division lines are introduced, every trajectory that steps inside the cell a' does so more than once before exiting. This is equivalent to introducing grammatical rules of length larger than 1. Introducing the division lines 2 and 3, we introduce additional cells but always have grammatical rules of length 1.

Based on these two principles, we have developed an algorithm for partitioning the phase space, which is described in technical detail in Ref. [6]. In Sec. V, we explain how this partition completely describes the path of each scattering trajectory.

IV. PARTITION OF THE DRIVEN-INVERTED GAUSSIAN

Following the basic two principles described above, one can show that the phase space of the driven inverted Gaussian is partitioned in five different cells [6]. We denote those five cells by the symbol values A,+, %, &, and C as shown in Fig. 9. As explained in Ref. [6], the cells A and C are defined on a finite hierarchical level, while the cells +, %, and & are defined on an infinite hierarchical level, see Figs. 9 and 10. The division lines for the system under consideration are shown in Figs. 9 and 10. Note that this partition of the phase space is general for all two-degree-of-freedom systems that are described by ternary horseshoes with development parameters (1, 1/3) [6,10]. We note that the so-called development parameter gives, approximately, the development stage of the horseshoe construction. The significance of this parameter is that it describes universal aspects of the horseshoe and ignores the details. That is, it determines the hyperbolic component of the invariant set, which is the important part for the scattering behavior, and neglects nonhyperbolic effects that are due to the Kolmogorov-Arnold-Moser (KAM) tori [13,15,16]. The nonhyperbolic effects appear at high levels of the hierarchy as tangencies, nontransversal intersections, between stable and unstable manifolds and have a very small effect on the scattering functions (see [15] for more details on tangencies between stable and unstable manifolds). For the values of the frequency and am-

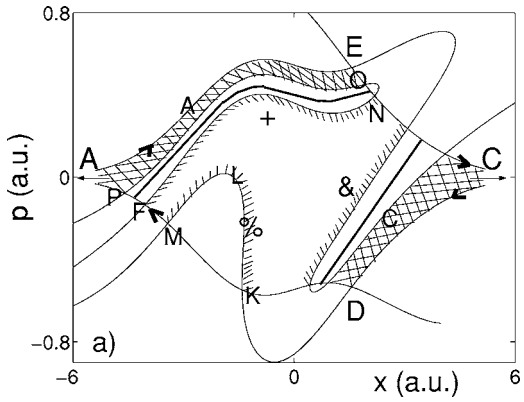

FIG. 9. The (1, 1/3) development stage of the asymmetric ternary horseshoe is partitioned into five cells: A,+, %, &, C. For more details, see Ref. [6].

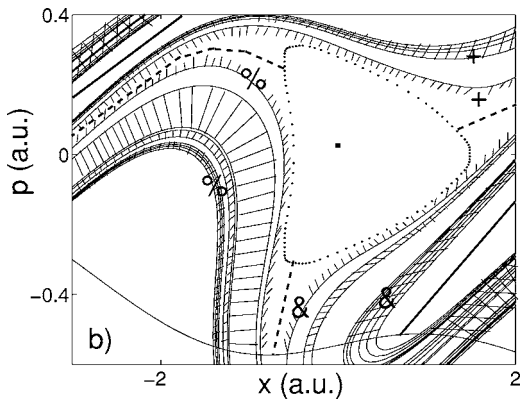

FIG. 10. Ternary asymmetric horseshoe with $\alpha's$ (1, 1/3). The thick broken lines show, schematically, where the division lines between the cells %, &, and + are in the limit of hierarchical level to infinity.

plitude of the driving field we chose, the nonhyperbolic effects become visible in the scattering functions at a hierarchical level 8 [10]. However, these nonhyperbolic effects take over and, thus, become important for hierarchical levels much higher than 8, in analogy to the system considered in Ref. [15]. We note that an exact description of the infinity of homoclinic tangencies is extremely complicated and beyond the scope of the present paper. The mathematically inclined reader can find some rigorous theorems on horseshoe-development scenarios (unfoldings of homoclinic tangencies) in [17,18] and references therein. In connection to the classification of Ref. [17], in this paper we consider a parameter range where, at least in the vicinity of the large KAM island, homoclinic tangencies persist; that is, we consider a case without nearby hyperbolic windows in the parameter space.

To derive the grammatical rules, one has to find how the images of the various cells map on to other cells. From Fig. 9, we find the grammatical rules to be

$$\mathbf{1:}A \to A,\&,C\ \mathbf{2:}\& \to C,\%\ \mathbf{3:}C \to C,\%\ \mathbf{4:}\% \to +,A$$
$$\mathbf{5:} + \to A,\&,C.$$

The next step is to encode the right and/or left branching trees in Figs. 5 and 6. To do so, one needs to know not only how a given cell maps to other cells but also the sequence in which the mapping takes place. We illustrate this last statement by explicitly showing how to encode the branching tree for scattering from the right, see Fig. 5. We choose to follow the unstable manifold of the outer fixed point C in Fig. 9 forward in time. As we follow the unstable manifold, we identify the order in which a segment of each partition cell maps to other cells. Note that in this section when we refer to a segment of a cell, we mean a segment of the unstable manifold that forms part of the boundary of this cell. For example, in Fig. 9, the segment CD of the C cell maps to C and %. These symbol values give us the encoding of the $n=1$ level of the branching tree, always from right to left, in Fig. 5. To find the symbol values of the $n=2$ level of the tree, from right to left, we follow the second-order tendril of the unstable manifold and note that the segment CD of the C cell maps to C and % and that the segment KLM of the cell % maps to + and A. Now, to encode the $n=3$ level of the part of the tree that branches out of % at level $n=1$ in Fig. 5, we follow the third-order tendril of the unstable manifold of the fixed point C and find that the segment FN of the + cell maps to A, &, and C cells, respectively, while the segment OP of the A cell maps to the C, &, and A cells, respectively. The encoding at level n of the tree that branches out of C at level $n=1$ in Fig. 5, is the same with the encoding of the whole tree at level $n-1$ due to self-similarity. For example, the encoding of the $n=3$ level of the tree that branches out of C at level $n=1$, is the same as the encoding of the whole tree at level $n=2$. In the same spirit, following forward in time the higher-order tendrils of the unstable manifold of C, we encode the higher hierarchical levels of the branching tree, as shown in Fig. 5. In analogy, one encodes the left-branching tree as shown in Fig. 6.

V. COMPLETE DESCRIPTION OF THE SCATTERING TRAJECTORIES AS A NATURAL RESULT OF OUR PARTITION

Our principles and strategy to partition incomplete horseshoes apply to any horseshoe defined on a two-dimensional domain. Our partition amounts to a *natural* way of partitioning the phase space if one is interested in the scattering properties of the system. That is, from our partition we can extract: (i) the number of times a scattering trajectory steps inside the fundamental region before it either reflects or transmits and (ii) the sequence of partition cells the trajectory steps in, in the area R. In the following, we explicitly show how we extract, from our partition, all the relevant information regarding scattering trajectories.

We illustrate, in Fig. 11, how to extract the relevant scattering information from our partition for the case when particles scatter in from the left. We start with a line of initial conditions in the left asymptotic region that intersects one complete outer tendril formed by the stable manifold of the fixed point C. The image of this line of initial conditions in each step of forward propagation in time stretches and continues to intersect the stable manifolds. Just before entering the area R, this line's image approaches the area R along the direction of the unstable manifold of the fixed point A and is denoted by line E in Fig. 11. We thus assume we have cleverly chosen the line of initial conditions to be a higher-order preimage of the line E. The part of the branching tree enclosed by a square in Fig. 6 describes the hierarchical structure of the intersections of the stable manifolds with the line of initial conditions E. Since all the scattering trajectories with initial conditions in the same interval of continuity of the scattering function have the same behavior, in the following, we concentrate on intervals of continuity and show how for each interval we obtain the relevant scattering information.

Before proceeding, let us briefly describe how we label intervals of continuity. In our construction of the branching trees, an interval of continuity of level $n+1$ is always in between two adjacent intervals that are still unresolved at level $n+1$. These unresolved intervals are represented by two entries (branches) of the branching tree on level $n+1$ that branch out of the same entry at level n. This entry of level n is represented by a symbol block (sequence of symbol values) X with length n. The above-mentioned two entries of level $n+1$ are labeled, using the symbol block X and the symbol values a and b, as Xa and Xb, respectively. We label the interval of continuity between these two unresolved structures by $X[a,b]$. Next, we describe how the $X[a,b]$ symbol sequence contains all the relevant information for trajectories with initial conditions in the $X[a,b]$ interval of continuity.

(i) The interval of continuity A [&,C], which is denoted as 1 in the branching tree in Fig. 6, corresponds to the segment of E that cuts through the first-order gap of the stable manifold of the fixed point A, denoted by the yellow segment labeled by 1 in Fig. 11. It is important to remember that each interval of continuity of the scattering function corresponds to a gap of the chaotic saddle. The first image of segment 1 is the yellow arc denoted by 1_1 which is already mapped

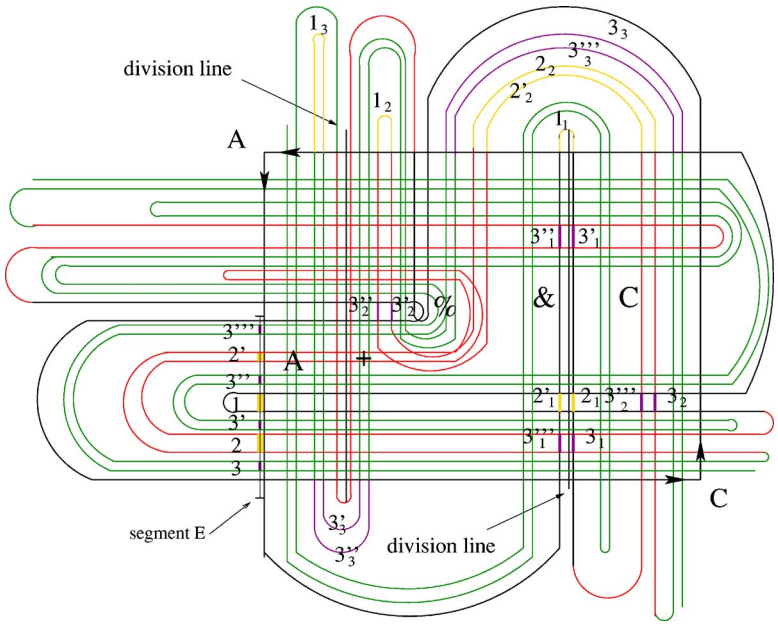

FIG. 11. (Color online) Schematic drawing of the (1, 1/3) development scenario of the driven inverted Gaussian. The black lines denote the local segments of the stable manifolds of points A and C and the first-order tendril of the unstable manifolds of the fixed points A and C. The red color is used to draw the second-order tendrils of the unstable manifolds of the fixed points A and C, while the green color is used to draw the third-order tendrils of the unstable manifolds of the fixed points A and C. The first image of the part of segment E labeled as 1 (yellow), is labeled 1_1 (yellow) and is the arc of the first-order tendril of the unstable manifold of A. In the schematic drawing, we have drawn the image 1_1 using yellow on top of the black (not shown) used to draw the first-order tendril. In the same way, we draw the images of all the intervals we consider. That is, the arcs of the unstable manifolds that are the images of the 1, 2, 2′, 3, 3′3″, and 3‴ segments of E are drawn with the same color as the one used for the corresponding segment. In reality, the images of the segments of line E are not on top of the arcs but slightly inside the corresponding gap. The reason is that the line E is ideally very close to the local segment of the unstable manifold of A but yet slightly outside the area R. In this figure, we just indicate the different partition cells. One has to compare to Fig. 9 to have a better picture of the different cells.

outside the area R. Its second image is the arc 1_2, with the next images getting closer and closer to the local segment of the unstable manifold of the fixed point A. Thus, the particles with initial conditions inside the interval of continuity A [&, C], are asymptotically thrown in from the left (fixed point A), do not step inside R, and reflect (escape to the left).

(ii) The interval of continuity AC[%,C], which is denoted as 2 in the branching tree in Fig. 6, corresponds to the segment of E that cuts through the second-order gap of the stable manifold of the fixed point A, denoted by the yellow segment labeled by 2 in Fig. 11. The first image of the segment 2 is the yellow segment 2_1, which is inside the partition cell C, the second image is the arc 2_2, which is already outside R. As for the case (i), the next images move closer to the unstable manifold of the fixed point A. Thus, the particles with initial conditions inside the interval of continuity AC[& C], are asymptotically thrown in from the left (fixed point A), step inside R once in the partition cell C and reflect to the left.

(iii) The interval of continuity A&[C,%], which is denoted as 2′ in the branching tree in Fig. 6, corresponds to the segment of E that cuts through the second-order gap of the stable manifold of the fixed point A, denoted by the yellow segment labeled by 2′ in Fig. 11. The first image of the 2′ segment is the yellow $2'_1$ segment, which is inside the partition cell &, the second image is the arc $2'_2$, which is already outside R. As for cases (i) and (ii), the next images move closer and closer to the unstable manifold of the fixed point A. Thus the particles with initial conditions inside the interval of continuity A&[C,%] are asymptotically thrown in from the left (fixed point A), step inside R once in the partition cell & and reflect to the left.

(iv) The interval of continuity ACC[%,C], which is denoted as 3 in the branching tree in Fig. 6, corresponds to the segment of E that cuts through the third-order gap of the stable manifold of the fixed point A, denoted by the purple segment labeled 3 in Fig. 11. The first image of the segment 3 is the purple 3_1 segment, which is inside the partition cell C; the second image is the purple segment 3_2, which is again inside the partition cell C. The third image of the 3 segment is the purple arc 3_3 and it is already outside R. As in the previous cases, the next images move along the direction of the unstable manifold of A. Thus, the particles with initial conditions inside the interval of continuity ACC[%,C] are asymptotically thrown in from the left (fixed point A), step inside R twice in the partition cell C and reflect to the left.

(v) The interval of continuity AC % [A, +], which is denoted as 3′ in the branching tree in Fig. 6, corresponds to the segment of E that cuts through the third-order gap of the stable manifold of the fixed point C, denoted by the purple segment labeled 3′ in Fig. 11. The first image of the 3′ segment is the purple $3'_1$ segment which is inside the partition cell C, the second image is the purple segment $3'_2$, and it is inside the partition cell %. The third image of the 3′ seg-

ment is the purple arc $3'_3$, and it is already outside R. The next images move closer and closer to the local segment of the unstable manifold of the fixed point C. Thus, the particles with initial conditions inside the interval of continuity $AC\%$ $[A,+]$, are asymptotically thrown in from the left, step inside R twice in the partition cells C and % and transmit to the right.

(vi) The interval of continuity $A\&\%[+,A]$, which is denoted as $3''$ in the branching tree in Fig. 6, corresponds to the segment of E that cuts through the third-order gap of the stable manifold of the fixed point C, denoted by the purple segment labeled $3''$ in Fig. 11. The first image of the $3''$ segment is the purple $3''_1$ segment which is inside the partition cell &, the second image is the purple segment $3''_2$ and it is inside the partition cell %. The third image of the $3''$ segment is the purple arc $3''_3$, and it is already outside R. As for case d, the next images move along the direction of the local segment of the unstable manifold of C. Thus, the particles with initial conditions inside the interval of continuity $A\&\%$ $[A,+]$, are asymptotically thrown in from the left (fixed point A), step inside R twice in the partition cells & and %, and transmit to the right.

(vii) The interval of continuity $A\&C$ $[C,\%]$, which is denoted as $3'''$ in the branching tree in Fig. 6, corresponds to the segment of E that cuts through the third-order gap of the stable manifold of the fixed point A, denoted by the purple segment labeled $3'''$ in Fig. 11. The first image of the $3'''$ segment is the purple $3'''_1$ segment which is inside the partition cell &, the second image is the purple segment $3'''_2$ and it is inside the partition cell C. The third image of the segment $3'''$ is the purple arc $3'''_3$, and it is already outside R. The next images move closer to the local segment of the unstable manifold of A. Thus, the particles with initial conditions inside the interval of continuity $A\&C$ $[C,\%]$, are asymptotically thrown in from the left (fixed point A), step inside R twice, in the partition cells & and C, and reflect to the left.

The pattern should be clear by now. The symbolic dynamics of an arbitrary interval of continuity labeled by $X[a,b]$ gives the following information for the scattering trajectories with initial conditions in this interval: The first symbol value of the symbol block X indicates the side the scattering trajectory comes in from. The remaining part of length $n-1$ of the symbol block X indicates that the trajectory steps $n-1$ times inside R. The sequence of the symbol values in the remaining part indicates the sequence of partition cells the scattering trajectory "steps" in inside the area R. Finally, from the symbol values inside the brackets $[a,b]$, one can determine whether the particle escapes asymptotically to the right or left. Specifically, for the development scenario of the system currently under consideration, the grammatical rules are such that at least one of the symbol values inside the brackets is either the fixed point A or C. If it is the symbol value A, for example, $[A, \&]$, then the segment of line E that corresponds to the initial conditions inside the interval of continuity labeled by $X[A,\&]$ approaches R from outside intersecting the stable manifolds of the fixed point C, and thus, once outside of R, the images of this interval of continuity get closer and closer to the local segment of the unstable manifold of C. If on the other hand, inside the brackets is the symbol value C, for example $X[C,\%]$, then the segment of line E that corresponds to the initial conditions inside the interval of continuity labeled by $X[C, \&]$ approaches R from outside intersecting the stable manifolds of the fixed point A, and thus, once outside of R the images of this interval of continuity get closer and closer to the local segment of the unstable manifold of A. Let us note that for different parameter values of the driven inverted Gaussian (or other systems), it can be the case that neither a nor b inside the brackets $[a,b]$ is one of the outer fixed points. Clearly, in this last case determining whether the particle scatters to the right or left is not as simple as checking which fixed point's symbol value is inside the brackets. We can again determine the direction the particle escapes, but additional instructions need to be introduced in this case.

VI. CONCLUSIONS

In the current work, we explain and motivate the basic two principles of a general scheme [6] of partitioning the phase space that is natural for scattering systems. This scheme is applicable to any system that can be cast into a two-dimensional Poincaré map. We have also shown, in detail, how our scheme of partitioning the phase space by using the unstable manifolds of the outer fixed points as division lines of the cells results in a natural partition from the scattering perspective. That is, the branching tree describing the scattering functions (which is what an asymptotic observer measure) and the branching tree, resulting from the partition of the phase space in the interaction region, are the same. That means that scattering trajectories with initial conditions in the same interval of continuity of a scattering function are described by the same symbol sequence.

[1] S. Smale, Bull. Am. Math. Soc. **73**, 747 (1967).

[2] P. Cvitanovic, G. H. Gunaratne, and I. Procaccia, Phys. Rev. A **38**, 1503 (1988).

[3] P. Grassberger and H. Kantz, Phys. Lett. **113**, 235 (1985); P. Grassberger, H. Kantz, and U. Moenig, J. Phys. A **22**, 5217 (1989).

[4] F. Christiansen and A. Politi, Phys. Rev. E **51**, R3811 (1995); F. Christiansen and A. Politi, Nonlinearity **9**, 1623 (1996).

[5] M. J. Feigenbaum, M. H. Jensen, and I. Procaccia, Phys. Rev. Lett. **57**, 1503 (1986); C. Beck and F. Schlogel, *Thermodynamics of Chaotic Systems* (Cambridge University Press, Cambridge, England, 1993); G. Karolyi and T. Tel, Phys. Rep. **290**, 125 (1997); B. Rückerl and C. Jung, J. Phys. A **27**, 6741 (1994).

[6] C. Jung and A. Emmanouilidou, Chaos **15**, 023101 (2005).

[7] A. Emmanouilidou and L. E. Reichl, Phys. Rev. A **65**, 033405

(2002).
[8] K. A. Mitchell, J. P. Handley, B. Tighe, A. Flower and J. B. Delos, Phys. Rev. Lett. **92**, 073001 (2004); Phys. Rev. A **70**, 043407 (2004).
[9] H. A. Kramers, *Collected Scientific Papers* (North-Holland, Amsterdam, 1956), p. 272.
[10] A. Emmanouilidou, C. Jung, and L. E. Reichl, Phys. Rev. E **68**, 046207 (2003).
[11] L. E. Reichl, *The Transition to Chaos in Conservative Classical Systems: Quantum Manifestations* (Springer-Verlag, Berlin, 1983).
[12] E. Ott, *Chaos in Dynamical Systems*, Cambridge University Press, Cambridge, England, 1993.
[13] C. Jung, C. Lipp, and T. H. Seligman, Ann. Phys. **275**, 151 (1999).
[14] D. Bigie, A. Leonard, and S. Wiggins, Nonlinearity **4**, 775 (1991).
[15] B. Rückerl and C. Jung, J. Phys. A **27**, 55 (1994).
[16] W. Breymann and C. Jung, Europhys. Lett. **25**, 509 (1994).
[17] I. Lugao Rios, Nonlinearity **14**, 431 (2001).
[18] J. Palis and J. C. Yoccoz, Comptes Rendus Mathematique **333**, 867 (2001).